Progress In Electromagnetics Research M, Vol. 24, 209–220, 2012

THE EFFECT OF POWER-LINE SAGGED CONDUCTORS ON THE EVALUATION OF THE DIFFERENTIAL VOLTAGE IN A NEARBY CIRCUIT AT GROUND LEVEL

J. A. Brandão Faria*

Instituto de Telecomunicações, Instituto Superior Técnico, Technical University of Lisbon, Av. Rovisco Pais, Lisboa 1049-001, Portugal

Abstract—Overhead-line power conductors do not run parallel to the ground; they actually sag between adjacent towers, defining catenary curves. However, in the analysis of inductive coupling phenomena between power lines and neighboring circuits, the standard approach to deal with the sag effect is to assign a constant average height to power line conductors. The purpose of this research is to assess the accuracy of such an ordinary procedure. To do that, two different approaches are developed in order to more accurately account for the sag effect: a pure segmentation method, and a corrected segmentation method which takes into consideration the real curvature of the sagged conductors. The latter, and novel, approach is compared with the other options. Calculations presented in this work utilize magnetic vector potential as an analysis tool.

1. INTRODUCTION

The consideration of conductors sag effect has been shown to be very important for the evaluation of the high-frequency wave propagation parameters of three-phase overhead lines [1]. In fact, line non-uniformity can give rise to resonant phenomena at certain critical frequencies. Also, the computation of magnetic fields produced by overhead power lines has been addressed in a number of papers [2–9] which include the effect of sagged conductors. This effect is especially important at mid span, because, there, the magnetic field is more intense, and the risk of exceeding the rulings [10] set by the International Commission of Non Ionizing Radiation Protection for safe public exposure to power-frequency magnetic fields is higher.

Received 30 April 2012, Accepted 24 March 2012, Scheduled 1 June 2012

* Corresponding author: Jose Antonio Marinho Brandão Faria (brandao.faria@ist.utl.pt).

Power-frequency inductive coupling between overhead power lines and neighboring circuits is a matter of concern in electrical engineering, as in the case of the coupling with railways, gas pipelines, and oil pipelines running at ground level, paralleling the power line route. The computation of the differential voltage between a pair of conductors involves the determination of a magnetic flux by surface integration of the whole magnetic induction field **B** along a line span length. As a result, the magnetic flux $\boldsymbol{\psi}$ includes small **B** contributions near to the power towers and high **B** contributions at mid span. Therefore, the integration process leading to $\boldsymbol{\psi}$ has an in-built "averaging" effect.

Is such an "averaging" effect adequately accounted by simply replacing the actual sagged conductors with horizontal conductors at average height? That is the question addressed in this paper.

In order to answer this particular question we consider just one single sagged conductor above a flat ground (avoiding the unnecessary complication arising from a three-phase line configuration). The problem to be handled is illustrated in Fig. 1. Conductors 1 and 2 (which may simulate a railway, a two-conductor gas pipeline or oil pipeline) are very near to the ground but are isolated from it. For simplification purposes we take $x_1(z) = x_2(z) \approx 0$. The separation between conductors 1 and 2 is denoted by $2a$. The lateral distance

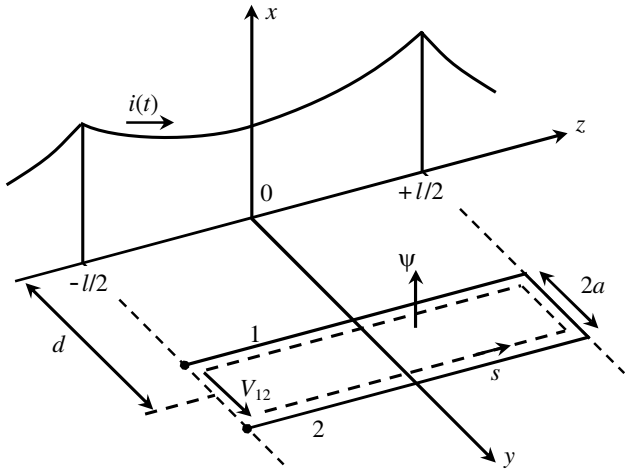

Figure 1. System geometry: A two-conductor circuit at ground level parallels a sagged overhead conductor running over a flat ground. The x coordinate of the sagged conductor describes a catenary curve $x(z)$. The x_1 and x_2 coordinates of conductors 1 and 2 are equal, $x_1(z) = x_2(z) \approx 0$. The differential voltage V_{12} is to be evaluated.

between the overhead conductor and the axis of the conductor pair is denoted by d. Our goal is to evaluate the differential voltage $\bar{V}_{12}$ between the pair of conductors at $z = -l/2$, assuming that at the opposite end ($z = l/2$), the two conductors are interconnected. Of course, in a longer circuit, occupying N_s line spans with total length $L = N_s\, l$ the differential voltage is N_s times bigger.

The height x of the current-carrying overhead conductor varies along the longitudinal coordinate z according to the catenary differential equation [4, 11],

$$\frac{d^2x}{dz^2} = \alpha\sqrt{1 + \left(\frac{dx}{dz}\right)^2}$$

where α is a dimensionless parameter which is related to conductor weight and stress. The exact solution to the preceding equation is of the hyperbolic-cosine type [4, 11]. However, for span lengths smaller than 500 m, the exact solution can be very accurately approximated by using the following parabolic law [1, 12],

$$x\,(z) = h_{\min} + s\left(\frac{2z}{l}\right)^2; \quad \text{for } -\frac{l}{2} \le z \le \frac{l}{2} \tag{1}$$

where l is the span length (distance between towers), $h_{\min}$ the minimum height (at mid span), and s the sag ($s = h_{\max} - h_{\min}$). Conductor's average height is determined through

$$h_{av} = \frac{1}{l}\int_{-l/2}^{l/2} x(z)\,dz = h_{\min} + \tfrac{1}{3}s \tag{2}$$

Maximum height $h_{\max}$ and minimum height $h_{\min}$ are related to h_{av} and s as follows

$$h_{\max} = h_{av} + \tfrac{2}{3}\,s, \quad h_{\min} = h_{av} - \tfrac{1}{3}\,s$$

In this work, we consider that all examples being examined and compared share the same average height h_{av} and the same span length l. The sag s will be the variable parameter. For analysis purposes the normalized sag ξ is introduced here

$$\xi = \frac{s}{s_{\max}} = \frac{s}{h_{\max}}; \quad 0 < \xi < 1 \tag{3}$$

Note that, in actual power lines, ξ can ordinarily be found in the range 0.4 to 0.5.

2. ZEROTH ORDER APPROACH

The usual approach to account for the catenary effect consists in modeling the real non-uniform line with variable height $x(z)$ by a virtual uniform line with constant height $x = h_{av}$.

The overhead conductor carries a sinusoidal current described by $i(t) = \text{Re}\ (\bar{I}\ e^{j\omega t})$, where $\bar{I}$ is the complex amplitude of $i(t)$. The complex amplitude of the magnetic vector potential external to the conductor and created by its own current is given by [13],

$$\bar{\mathbf{A}} = \bar{A}\ \vec{e}_c, \quad \bar{A} = \frac{\mu_0}{2\pi}\bar{I}\ln\left(\frac{1}{r}\right) + \bar{A}_0\ , \quad \vec{e}_c = \ \vec{e}_z \tag{4}$$

where $\vec{e}_c$ is the unit vector oriented according to the reference direction assigned to $i(t)$, r is the radial distance, and $\bar{A}_0$ is an arbitrary constant. The magnetic induction field can be determined from (4) using $\bar{\mathbf{B}} = \nabla \times \bar{\mathbf{A}}$, yielding $\bar{\mathbf{B}} = \mu_0\bar{I}/(2\pi r)\ \vec{e}_\phi$ [13, 14].

Application of Faraday's law to a rectangular path $\vec{s}$ coinciding with the circuit formed by the conductors #1 and #2 at ground level (see Fig. 1) yields the differential voltage $\bar{V}_{12}$

$$\oint \bar{\mathbf{E}} \bullet d\bar{s} = \bar{V}_{12} = -j\omega \overbrace{\int_{S_s} \bar{\mathbf{B}} \bullet \mathbf{n}\, dS}^{\bar{\psi}} = -j\omega \oint \bar{\mathbf{A}} \bullet d\bar{s}$$

$$= j2\omega \int_{-l/2}^{0} \left(\bar{A}_1 - \bar{A}_2\right) dz \tag{5}$$

where $\bar{A}_1 = \bar{A}(x = 0,\ y = d - a)$ and $\bar{A}_2 = \bar{A}(x = 0,\ y = d + a)$.

The magnetic induction field $\mathbf{B}$ in (5) is the result of the superposition of two contributions. The contribution from the overhead conductor current and the contribution from ground return currents.

However, for power frequencies, the latter contribution is negligibly small. In fact, using Dubanton's complex ground plane approach [15–17], the ground return current can be simulated by means of a fictitious current filament $(-\bar{I})$ located deep inside the ground at a complex distance $(2\bar{p} + h_{av})$ from the ground/air interface, where, for a nonmagnetic ground, $\bar{p}$ is given by

$$\bar{p} = \frac{1}{\sqrt{j\omega\sigma_G\mu_0}} \tag{6}$$

For $f = 50\,\text{Hz}$ and for an average ground with conductivity $\sigma_G = 0.01\,\text{S/m}$ we find $|2\bar{p}| > 1\,\text{km}$.

Therefore, in what follows, we will always neglect the field originated by ground currents.

With the help of Fig. 2 (a cross section of the conductor system) we can determine the difference $(\bar{A}_1 - \bar{A}_2)$ in (5)

$$\bar{A}_1 - \bar{A}_2 = \frac{\mu_0}{4\pi}\bar{I}\ln\left(\frac{r_2}{r_1}\right)^2 = \frac{\mu_0}{4\pi}\bar{I}\ln\left(\frac{h_{av}^2 + (d+a)^2}{h_{av}^2 + (d-a)^2}\right) \tag{7}$$

Since (7) does not depend on z, we obtain from (5) the zeroth order approximation for the differential voltage

$$\bar{V}_{12} = \bar{Z}_M^{(0)}\bar{I}\ , \quad \bar{Z}_M^{(0)} = \frac{j\omega\mu_0 l}{4\pi}\ln\left(\frac{h_{av}^2 + (d+a)^2}{h_{av}^2 + (d-a)^2}\right) \tag{8}$$

It should be noted that, as expected, the 0th order approximation for the mutual impedance $\bar{Z}_M$ is zero for $d = 0$. In order to see where $\bar{V}_{12}$ is maximum we may solve the equation $\partial Z_M/\partial d = 0$, which yields

$$d = d_0 = \sqrt{h_{av}^2 + a^2} \quad \rightarrow \quad \bar{Z}_{M_{\max}}^{(0)} = \frac{j\omega\mu_0 l}{4\pi}\ln\left(\frac{d_0 + a}{d_0 - a}\right) \tag{9a}$$

When $a \ll h_{av}$, as it is normally the case, the results in (9a) simplify

$$d_0 \approx h_{av}, \quad \bar{Z}_{M_{\max}}^{(0)} \approx \frac{j\omega\mu_0 S}{4\pi h_{av}} \tag{9b}$$

where $S = 2al$ is the area of the rectangular loop defined by conductors #1 and #2 (see Fig. 1).

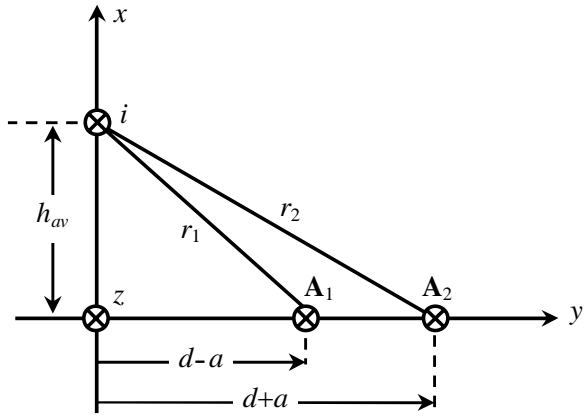

Figure 2. Geometrical distances involved in the computation of the magnetic vector potential along conductors 1 and 2. In the general case, height h_{av} must be replaced by $x(z)$ in (1).

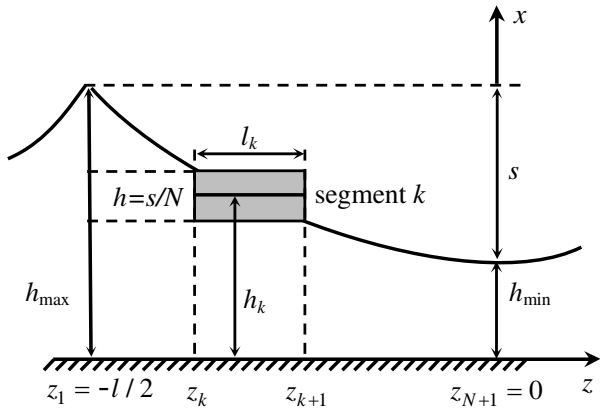

Figure 3. Identification of the horizontal segment k of length l_k at height h_k.

3. FIRST ORDER APPROACH

The first order approach utilizes the segmentation method, or staircase approximation [1], where the overhead conductor is modeled by means of a chain of $2N$ elemental uniform segments parallel to the ground, each segment carrying a current $\bar{I}$.

The average height of each segment gradually changes according to the variation law for $x(z)$ in (1). The number of segments associated with the discretization process depends on the sag value. The greater the sag the greater the number of segments required. Each step of the stair case approximation has a constant step height $\Delta h = s/N$, where N is the chosen number of segments in the range to $z = -l/2$ to $z = 0$.

As shown in Fig. 3 the uniform conductor corresponding to the generic segment k (with k from 1 to N) is characterized by an average height h_k and length l_k calculated according to (1), and given by:

$$l_k = z_{k+1} - z_k = \frac{l}{2}\left\{\sqrt{1-\frac{k-1}{N}} - \sqrt{1-\frac{k}{N}}\right\} \tag{10}$$

and

$$h_k = \frac{1}{l_k}\int_{z_k}^{z_{k+1}} x\,(z)dz = h_{av} + \frac{\Delta h}{3}\left(1+N-2k+\sqrt{(N-k)\,(N-k+1)}\right) \tag{11}$$

with $z_1 = -l/2$ and $z_{N+1} = 0$.

It is worth mentioning that when k increases (i.e., as one gets near to mid span) the length of the segments progressively enlarges, so as to keep Δh constant from segment to segment.

Now, contrary to the situation in (7), the difference $(\bar{A}_1 - \bar{A}_2)$ depends on z, and varies from segment to segment. Therefore, the result in (5) should be changed to

$$\bar{V}_{12} = j2\omega \int_{-l/2}^{0} (\bar{A}_1 - \bar{A}_2)\, dz = j2\omega \sum_{k=1}^{N} (\bar{A}_1 - \bar{A}_2)_k\, l_k \tag{12}$$

where

$$\left(\bar{A}_1 - \bar{A}_2\right)_k = \frac{\mu_0}{4\pi} \bar{I} \ln\left(\frac{h_k^2 + (d+a)^2}{h_k^2 + (d-a)^2}\right) \tag{13}$$

Hence, the 1st order approximation for the mutual impedance $\bar{Z}_M$ is now found to be

$$\bar{Z}_M^{(1)} = \frac{j\omega\mu_0}{2\pi} \sum_{k=1}^{N} \ln\left(\frac{h_k^2 + (d+a)^2}{h_k^2 + (d-a)^2}\right) l_k \tag{14}$$

4. SECOND ORDER APPROXIMATION

In the stair case approximation developed in Section 3, all the horizontal segments carry the same z-oriented current $\bar{I}$. However, because of sagging, the real segments are not horizontal. As shown in Fig. 4 the current in the curved conductor can be broken down into two components: a x component $\bar{I}_x$ and a z component $\bar{I}_z = \bar{I}\cos\theta$, where θ varies with z along the line.

Note that $\bar{I}_x$ cannot give rise to a z-component of the magnetic vector potential; hence, $\bar{I}_x$ does not contribute to the evaluation of the differential voltage $\bar{V}_{12}$.

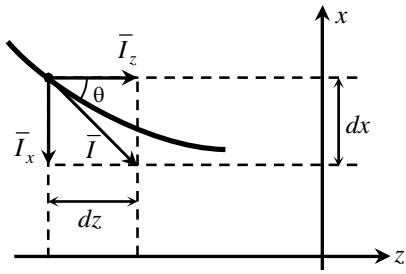

Figure 4. Horizontal and vertical components of $\bar{I}$ due to sagged conductor's curvature. The angle θ is such that $\tan\theta = dx/dz$.

The angle $\theta(z)$ can be determined using (1) — see Fig. 4,

$$\frac{dx}{dz} = \tan\theta(z) = \frac{z}{u} \quad \rightarrow \quad \cos\theta(z) = \frac{1}{\sqrt{1+(z/u)^2}} \tag{15}$$

where

$$u = l^2/(8s) \tag{16}$$

The segmentation method can be improved by assigning a z-oriented current $\bar{I}_k = \bar{I}\cos\theta_k$ to each segment, from $k = 1$ to N, where $\cos\theta_k$ is the average value of $\cos\theta(z)$ in the interval $[z_k,\ z_{k+1}]$ of length l_k:

$$\cos\theta_k = \frac{1}{l_k}\int_{z_k}^{z_{k+1}} \frac{dz}{\sqrt{1+(z/u)^2}} = \frac{u}{l_k}\ln\left(\frac{(z_k+l_k)+\sqrt{(z_k+l_k)^2+u^2}}{z_k+\sqrt{z_k^2+u^2}}\right) \tag{17}$$

Accordingly, the result in (13) changes to

$$\left(\bar{A}_1 - \bar{A}_2\right)_k = \frac{\mu_0}{4\pi}\bar{I}\ln\left(\frac{h_k^2+(d+a)^2}{h_k^2+(d-a)^2}\right)\cos\theta_k$$

and, the 2nd order approximation for the mutual impedance $\bar{Z}_M$ is now obtained as

$$\bar{Z}_M^{(2)} = \frac{j\omega\mu_0}{2\pi}\sum_{k=1}^{N}\ln\left(\frac{h_k^2+(d+a)^2}{h_k^2+(d-a)^2}\right) l_k\cos\theta_k \tag{18}$$

5. COMPUTATION RESULTS

For illustration purposes we took the following fixed parameters:

$$h_{av} = 15\,\text{m}, \quad l = 300\,\text{m}, \quad a = 75\,\text{cm}, \quad f = 50\,\text{Hz} \tag{19}$$

With regard to the segmentation methods, we utilized a discretization degree as refined as $\Delta h/s \approx 5\%$ (we also experimented with $\Delta h/s \approx 1\%$ but no visible alterations were detected).

Firstly, as far as the sagged overhead conductor is concerned, we have assigned a typical value of 0.4 to the normalized sag ξ defined in (3). This translates into $h_{\max} = 20.45\,\text{m}$, $h_{\min} = 12.27\,\text{m}$, and $s = 8.18\,\text{m}$. The rms current in the sagged conductor is 2 kA. Secondly, we considered a receiving circuit 3 km long (corresponding to 10 line spans, $N_s = 10$). The circuit, placed at ground level, is positioned at a distance d away from the sagged conductor. We let the distance d to vary from $d = 0$ to $d = 2h_{av} = 30\,\text{m}$.

Figure 5 depicts the graphic evolution of $(V_{12})_{rms}$ against the varying parameter d/h_{av}, considering the application of the 0th, 1st, and 2nd order approaches developed in this work.

It can be seen that maximum V_{12} occurs when $d \approx h_{av}$, with $(V_{12})_{\max} \approx 19\,\mathrm{V}$. These results comply with the estimation results derived in (9).

The results obtained by using the 0th order approach (horizontal conductor at average height above the ground) are slightly smaller than those predicted using the 1st and 2nd order approaches. The curves describing the latter approaches are practically indiscernible from each other.

Differential voltages in Fig. 5 were obtained at 50 Hz (and $I_{rms} = 2\,\mathrm{kA}$). According to (12), should the product ωI_{rms} increase by a given scale factor, the differential voltage would increase by the same factor.

In order to more exactly quantify the errors introduced by using the 0th and 1st order approaches, we defined the following mutual impedance error functions, which do not depend on ωI_{rms}, but do vary with the sag value

$$\mathrm{Error}_{02}(\xi) = \frac{\left|\bar{Z}_M^{(0)}(\xi)\right| - \left|\bar{Z}_M^{(2)}(\xi)\right|}{\left|\bar{Z}_M^{(2)}(\xi)\right|} \times 100\,\% \tag{20}$$

$$\mathrm{Error}_{12}(\xi) = \frac{\left|\bar{Z}_M^{(1)}(\xi)\right| - \left|\bar{Z}_M^{(2)}(\xi)\right|}{\left|\bar{Z}_M^{(2)}(\xi)\right|} \times 100\,\% \tag{21}$$

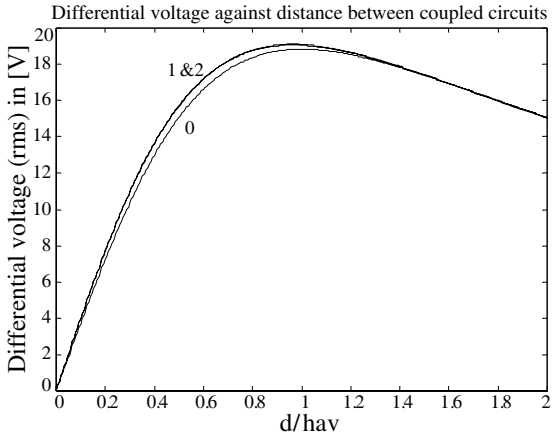

Figure 5. Differential voltage against distance between coupled circuits. Curves 0, 1 and 2 refer, respectively, to the 0th, 1st, and 2nd order approaches.

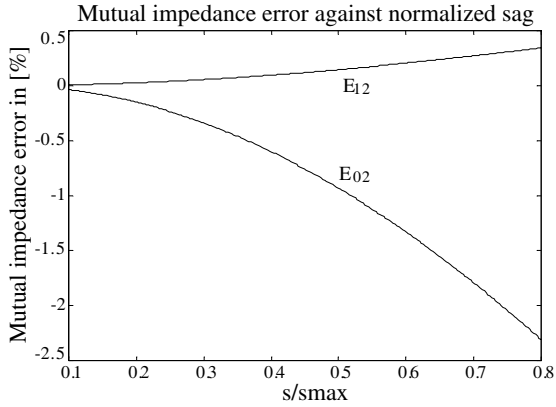

Figure 6. Errors of the 0th and 1st order approaches when compared with the accurate 2nd order approach (curves E02 and E12, respectively).

The receiving circuit was placed at $d = h_{av}$ and the normalized sag $\xi = s/s_{\max}$ was allowed to vary in the range 0.1 to 0.8. Computed results are shown in Fig. 6.

As expected, the error magnitude is higher for the 0th order approach: $|\text{Error}_{02}| > |\text{Error}_{12}|$. While the 0th order approach underestimates the differential voltage, the 1th order approach overestimates it. This is so, because $\left|\bar{Z}_M^{(0)}\right| < \left|\bar{Z}_M^{(2)}\right| < \left|\bar{Z}_M^{(1)}\right|$; the latter inequality results from the influence of $\cos\theta_k < 1$ in (18).

For ordinary situations, where ξ is in the interval 0.4 to 0.5, it can be observed that errors incurred by using the 0th order approach are smaller than 1%. Therefore, as far as the evaluation of the differential voltage is concerned, our conclusion is that the 0th order approach is quite adequate — there is no justification to utilize the more elaborated and time-consuming segmentation methods.

Note: Commercialized 3D full-wave simulators could have been used to compute the differential voltage V_{12} and, provided that their codes have no bugs, we are certain that they would lead to the same conclusion we have reached using the segmentation method and direct field analysis. The utilization of full-wave simulators produces output results that are opaque from a utilizer point of view, not giving him any physical interpretation of the phenomena being simulated; full-wave simulators should and must be used to solve problems with very complicated geometries for which direct analytical approaches are very difficult or even impossible to be implemented — which, clearly, is not the present case.

6. CONCLUSION

This work addressed the question if the ordinary approach of substituting a horizontal conductor at average height above the ground for a real sagged conductor would be a fairly accurate procedure as far as the evaluation of differential voltages induced in neighboring circuits is concerned. To that end two segmentation methods were developed, one where the sagged conductor was broken down into a number of uniform segments, and another one where, in addition, the local curvature of the sagged conductor was accounted for. Results produced by both segmentation methods showed that the improvement in the calculation of differential voltages was not significant. Errors incurred by using the ordinary approach are smaller than 1% for typical sag values.

ACKNOWLEDGMENT

The Portuguese Foundation for Science and Technology (FCT) sponsored this work.

REFERENCES

1. Faria, J., "High frequency modal analysis of lossy non-uniform three-phase overhead lines taking into account the catenary effect," *Euro. Trans. Electr. Power*, Vol. 11, No. 3, 195–200, 2001.
2. Memari, A. R. and W. Janischewskyj, "Mitigation of magnetic field near power lines," *IEEE Trans. Power Del.*, Vol. 11, 1577–1586, 1996.
3. Dahab, A. A., F. K. Amoura, and W. S. Abu-Elhaija, "Comparison of magnetic-field distribution of noncompact and compact parallel transmission-line configurations," *IEEE Trans. Power Del.*, Vol. 20, 2114–2118, 2005.
4. Budnik, K. and W. Machczynski, "Contribution to studies of the magnetic field under power lines," *Euro. Trans. Electr. Power*, Vol. 16, 345–354, 2006.
5. Faria, J. and M. Almeida, "Accurate calculation of magnetic-field intensity due to overhead power lines with or without mitigation loops with or without capacitor compensation," *IEEE Trans. Power Del.*, Vol. 22, 951–959, 2007.
6. Faria, J. and M. Almeida, "Computation of transmission line magnetic field harmonics," *Euro. Trans. Electr. Power*, Vol. 17, 512–525, 2007.

7. Maung, N. and X.-B. Xu, "Broadband PLC radiation from a power line with sag," *PIERS Online*, Vol. 3, No. 6, 767–769, 2007.
8. Al Salameh, M. S. H. and M. A. S. Hassouna, "Arranging overhead power transmission line conductors using swarm intelligence technique to minimize electromagnetic fields," *Progress In Electromagnetics Research B*, Vol. 26, 213–236, 2010.
9. Moro, F. and R. Turri, "Accurate calculation of the right-of-way width for power line magnetic field impact assessment," *Progress In Electromagnetics Research B*, Vol. 37, 343–364, 2012.
10. International Commission of Non Ionizing Radiation Protection, "Guidelines for limiting exposure to time-varying electric, magnetic and electromagnetic fields," *Health Phys.*, Vol. 74, 494–522, 1988.
11. Piskunov, N., *Differential and Integral Calculus*, MIR Publishers, Moscow, 1977.
12. Correia de Barros, M., "Computation of line parameters: Theoretical background" *European EMTP Short Course.*, Kul, Belgium, July–August 1984.
13. Solymar, L., *Lectures on Electromagnetic Theory*, Oxford University Press, Oxford, UK, 1984.
14. Faria, J., *Electromagnetic Foundations of Electrical Engineering*, Wiley, Chichester, UK, 2008.
15. Dubanton, C., "Calcul approché des parametres primaires et secondaire d'une ligne de transport," *EDF Bulletin de la Direction des Etudes et Recherches*, Vol. 1, 53–62, 1969.
16. Deri, A., G. Tevan, A. Semlyen, and A. Castanheira, "The complex ground return plane: A simplified model for homogeneous and multi-layer earth return," *IEEE Trans. Power App. Syst.*, Vol. 100, 3686–3693, 1981.
17. Deri, A. and G. Tevan, "Mathematical verification of Dubanton's simplified calculation of overhead transmission line parameters and its physical interpretation," *Arch. Elektrotechnik*, Vol. 63, 191–198, 1981.